Diffusion Impedance and Space Charge Capacitance in the Nanoporous Dye-Sensitized Electrochemical Solar Cell†

Klaus Schwarzburg* and Frank Willig

Hahn-Meitner-Institut, Glienicker Strasse 100, 14109 Berlin, Germany

Received: November 8, 2002

A measurement of the true space charge capacitance of the dye-sensitized solar cell (DSC) is presented here that shows good qualitative agreement with our simple physical model presented earlier [*J. Phys. Chem. B* **1999**, *103*, 5743]. This space charge capacitance does not show any significant increase with rising applied forward bias. In contrast, recently published impedance data show an exponential increase of the apparent capacitance [*J. Phys. Chem B* **2000**, *104*, 2044]. A simple analytical model is presented here for the impedance behavior of the DSC under forward bias revealing its nature as diffusion effect. The prediction of this model shows good qualitative agreement with the experimental results.

I. Introduction

This paper addresses the capacitive behavior of the nanoporous dye-sensitized electrochemical solar cell (DSC).[3,4] First, a direct measurement is presented here of the true space charge capacitance in the DSC. The value of the latter is determined from pulsed time-resolved photocurrent measurements.[5,6] It shows good qualitative agreement with the predictions of our simple physical model.[1] Second, a simple physical model is presented here for the impedance of the DSC under forward bias. The predictions of this model are in good qualitative agreement with recently published experimental results on the capacitive behavior of the DSC under forward bias.[2] These authors and also Dloczik et al.[7] have published impedance data that show an exponential increase of the cell's apparent capacitance with increasing forward bias. A similar effect has been observed by Zaban et al.[8] However, in the latter work, the electrolyte did not contain any active redox species, and it is unclear how these data are related to the impedance behavior of the working cell. Lagemaat et al.[2] conclude that the observed bias dependence of the capacitance measured as impedance under forward bias would refute our model for the space charge capacitance and photovoltage in the DSC.[1] According to our model, the build-up of the photovoltage occurs at the SnO_2/TiO_2 back contact. As in any other physical system, the corresponding electrical double layer is associated with a space charge capacitance. This capacitance is defined in terms of electrostatics governed by Poisson's equation. It would indeed be hard to explain how this space charge layer capacitance[1] could increase exponentially with the applied bias. Zaban et al.'s notion[8] is even less compatible with our model. These authors have considered a degenerate, metal-like TiO_2 network with a high surface area and thus a very high capacitance. It will be shown here that a much simpler explanation is available for the observed impedance behavior not contradicting our model at all. It dates back to the early days of semiconductor physics, when Shockley developed in the year 1949 his theory of pn-junctions.[9] He calculated the electrical impedance caused by diffusing screened minority carriers in dependence on the applied bias. The outcome of this calculation is a diffusion capacitance that scales with the applied forward current. This capacitance is in parallel with the space charge capacitance and is usually dominating the capacitive behavior of the junction under forward current flow. Similar theories are known in electrochemistry, in which the diffusion impedance is also known as "Warburg" impedance. The capacitive effect in the diffusion impedance of both pn-junction and electrochemical cell is not related to an electrostatic capacitance. It will be shown here that the capacitive effect seen in the impedance of the DSC can be derived from the same basic physical model known for a long time for the pn-junction. The simple analytical model presented here for the diffusion impedance of the DSC is in very good qualitative agreement with the reported experimental behavior of the DSC.[2]

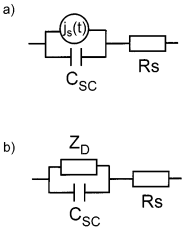

Figure 1. Equivalent circuit for (a) time-resolved photocurrent measurements and (b) impedance measurements of a diode. C_{SC} represents capacitance of the space charge region where charge separation is occurring; R_S is the cell's series resistance; $j_s(t)$ is a current source that contains the physical model for the transport of the charge carriers.[6,5] Z_D is the impedance related to the physics of the diode equation. In the simplest case, Z_D is the differential resitance of the dc diode equation, that is, a pure ohmic resistor. In the model presented here, it stands also for the diffusion impedance of the junction (see text).

II. Space Charge Capacitance, C_{SC}

Figure 1a shows the simplest generic equivalent circuit for a solar cell under transient illumination. It consists of a series resistance (R_s), a space charge capacitance (C_{SC}), and a current source ($j_s(t)$) that represents the time-dependent photoinduced

† This manuscript was originally received on November 9, 2000. It was deactivated and received a new receipt date because of untimely resubmission.

10.1021/jp022395+ CCC: $25.00
Published on Web 03/26/2003

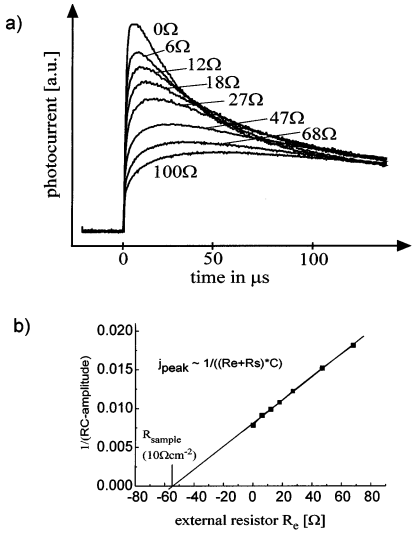

Figure 2. Photocurrent transients of the DSC (a) with different series resistors inserted into the external circuit and (b) plot of the inverse peak currents of panel a vs magnitude of the external resistor.

displacement current in the space charge region. As long as $j_s(t)$ is only a charging current, that is, $j_s(t)$ does not change sign, the decay time of the cell is limited by the *RC* time constant, $\tau = R_s C_{SC}$, formed by the space charge capacitance and the series resistance. Figure 2a shows the electrical response of the DSC under illumination with a nanosecond laser pulse (533 nm, 10 ns fwhm) for different magnitudes (parameter values) of an extra ohmic resistor in the electrical circuit. The photocurrent transient is continuing into the millisecond time range. This later time window is not shown here because it is not affected by the presence of the additional series resistor. The reciprocal peak amplitude of the photocurrent transient scales linearly with the additional series resistance (Figure 2b), and the extrapolation to $1/j_{peak} = 0$ gives the series resistance of the cell. This is the typical behavior corresponding to low-pass *RC* shaping if the duration of the internal current ($j_s(t)$) is shorter than the *RC* time constant of the circuit.[6,5] The series resistance obtained from the photocurrent transients is identical to the value obtained from the dark *I*−*V* curve. From the fit to the decay of the transients and inserting the series resistance, one obtains the cell capacitance in the range 5 μF/cm^2. It varies among different cells but remains always in this order of magnitude. This value for the capacitance is in good agreement with the prediction of the recently published electrostatic model.[1] In contrast to the behavior of the impedance,[2,8] there is no significant increase in the measured *RC* time constant and thus in the value of the capacitance C_{SC} if a strong forward bias is applied to the cell. A detailed discussion of the photocurrent transient in the DSC will be presented elsewhere.[10]

III. Diffusion Impedance, Z_D

The simplest approach to modeling the impedance behavior of a diode-like device (Figure 1b) is realized via an equivalent circuit that consists of passive elements only: a series resistance (R_s), a space charge capacitance (C_{SC}), and the impedance (Z_D) in Figure 1b, which is represented by just a resistance in parallel to the capacitance. This way one can model the linearized diode *I*−*V* conductance. In many cases, this approach is sufficient for obtaining a satisfactory approximation of the impedance under reverse bias conditions. However, it is well-known for solid-state semiconductor diodes that this approximation fails under forward bias conditions. Shockley[9] has shown for a pn junction under forward bias that the ac behavior of the minority carriers gives a capacitive-like response that increases exponentially with applied forward bias. Under strong forward bias, this minority carrier diffusion capacitance becomes larger than the true space charge capacitance and is dominating the impedance behavior. It is shown here that the same effect is responsible for the reported[2] exponential increase in the apparent capacitance with applied forward bias in the dye-sensitized cell.

Consider a small harmonic variation in the applied potential $\Delta V \exp(i\omega t)$. This change in potential will result in a current flow across the SnO_2/TiO_2 interface to establish the corresponding electron concentration on the TiO_2 side according to

$$n|_{x=0} = n_0 \, e^{\beta(V_0+\Delta V \, e^{i\omega t})} \approx n_0 \, e^{\beta V_0}(1 + \beta \Delta V \, e^{i\omega t}) \qquad (1)$$

$\beta = q/(k_b T)$ contains the Boltzmann factor, n_0 is the equilibrium electron concentration without applied bias, and V_0 is the additional dc bias. The linear approximation in eq 1 is valid if $\Delta V \ll k_b T/q$. The electron concentration at the SnO_2/TiO_2 interface ($x = 0$) will adjust very rapidly. The stationary state is reached after the spatial distribution of electrons has adjusted in the whole TiO_2 film to the new interface concentration. It is well established by photoimpedance measurements[11] that the motion of electrons in the nanometer-sized TiO_2 matrix surrounded by a conductive electrolyte solution can be described reasonably well by a diffusion equation, provided the change in electron concentration is small compared to the stationary concentration. Thus, for a sufficiently small harmonic bias, one can assume that the flow of screened electrons is governed by the continuity equation for neutral diffusing particles with a lifetime τ and a diffusion constant *D*:

$$\frac{\partial n(x,t)}{\partial t} = D\frac{\partial^2 n(x,t)}{\partial x^2} - \frac{n(x,t) - n_0}{\tau} \qquad (2)$$

The explicit time dependence can be removed by the ansatz:

$$n(x,t) = \tilde{n}(x) \, e^{i\omega t} \qquad (3)$$

Equation 2 then transforms into a diffusion equation with a complex lifetime, τ^*:

$$D\frac{\partial^2 \tilde{n}(x,t)}{\partial x^2} - \frac{\tilde{n}(x,t)}{\tau^*} = 0 \qquad \tau^* = \frac{\tau}{1 + i\omega\tau} \qquad (4)$$

We set the boundary condition at the SnO_2/TiO_2 interface ($x = 0$) according to eq 1 and assume a reflecting boundary at the electrolyte side of the electrode ($x = L$):

$$\tilde{n}|_{x=0} = n_0 \beta \Delta V \, e^{\beta V_0} e^{i\omega t} \qquad \frac{\partial \tilde{n}}{\partial x}|_{x=L} = 0 \qquad (5)$$

The following solution for the current $j(t)$ is found:

$$j(t) = qD\frac{dn}{dx}\Big|_{x=0} = \frac{qDn_0\beta\Delta V \, e^{\beta V_0} \, e^{i\omega t}}{L_D}\sqrt{1 + i\omega\tau}\tanh\left(\frac{L}{L_D^*}\right) \qquad (6)$$

the real and complex diffusion length, L_D and L_D^* being

$$L_D = \sqrt{D\tau} \qquad L_D^* = \sqrt{\frac{D\tau}{1 + i\omega\tau}} \qquad (7)$$

The complex diffusion admittance, *Y*, is obtained by dividing

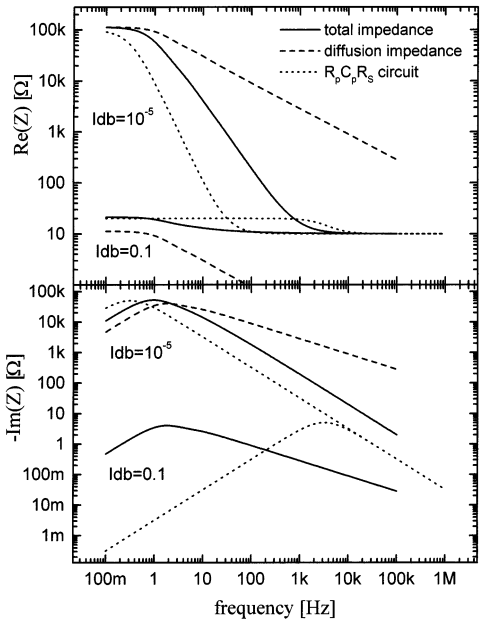

Figure 3. Calculated real and imaginary part of the total, of the diffusion, and of the $R_PC_PR_s$ impedance. The total impedance includes the diffusion impedance, as well as the space charge capacitance (C_{SC}) and the series resitance (R_s) according to the circuit in Figure 1b. $L = 10^{-3}$cm; $D = 5 \times 10^{-6}$ cm^2/s, $\tau = 0.1$ s, $C_{SC} = 5$ μF/cm^2; $R_s = 10$ Ω/cm^2. Two sets of curves are shown corresponding to the case of a strong forward current ($I_{db} = 0.1$ A/V/cm^2) and of a small current ($I_{db} = 10^{-5}$ A/V/cm^2). For the $R_PC_PR_s$ curves, $R_P = 10$ Ω/cm^2 was used for $I_{db} = 0.1$ and $R_P = 10^5$ Ω/cm^2 for $I_{db} = 10^5$.

$j(t)$ by the applied harmonic voltage, $\Delta V \exp(i\omega t)$. When $I_d(V_0)$ is substituted for the term $qDn_0\, e^{\beta V_0}/L_D$, which represents the stationary diffusion current, the admittance reads

$$Y_D = \frac{1}{Z_D} = I_d(V_0)\beta\sqrt{1 + i\omega\tau}\,\tanh\left(\frac{L}{L_D^*}\right) \qquad (8)$$

If the TiO_2 film is thick compared to the diffusion length ($L \gg L_D$), the tanh term is 1, and the result is identical to the admittance obtained for one side of the pn-junction diode.[9] Because Y_D is proportional to the stationary dc dark current $I_d(V_0)$, the diffusion admittance increases exponentially with the forward bias. Note that the admittance increases with the ratio L/L_D^*, and thus the diffusion capacitance increases with the TiO_2 film thickness, as has been found in the experiment.[8]

To calculate the total impedance, Z, of the cell, the series resistance, R_s, and the space charge capacitance, C_{SC}, have to be added (Figure 1b). The behavior of the diffusion admittance at very high and low frequencies can by be found by separating the dominant square root term into its real and imaginary parts:

$$\sqrt{1 + i\omega\tau} = \sqrt{\sqrt{1 + \omega^2\tau^2} + 1} + i\sqrt{\sqrt{1 + \omega^2\tau^2} - 1}$$
$$\xrightarrow{\omega\to\infty} \sqrt{\omega\tau} + i\sqrt{\omega\tau}$$
$$\xrightarrow{\omega\to 0} \sqrt{2} + \frac{i\omega\tau}{\sqrt{2}} \qquad (9)$$

If we view the diffusion admittance as parallel conductance and capacitance, $Y = G + i\omega C$, both C and G become constants at low frequencies, $\omega\tau \ll 1$, while at high frequencies, the diffusion capacitance vanishes as $1/\sqrt{\omega}$. Thus, the diffusion capacitance becomes most important at low frequencies and under forward bias conditions. Figure 3 shows the calculated real and imaginary

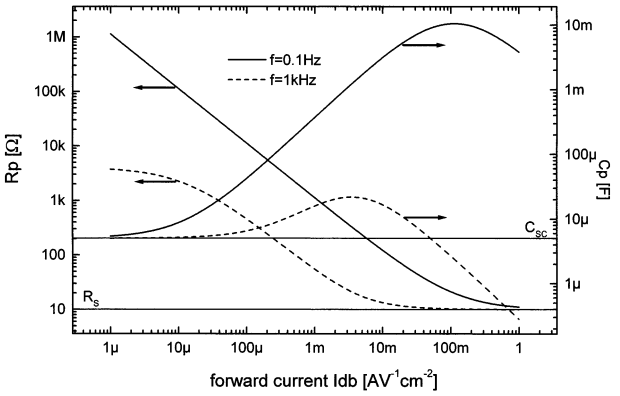

Figure 4. Calculated dependence on the magnitude of the forward current for the equivalent parallel resistance and for the equivalent apparent capacitance, both calculated from the total impedance. Same parameter values as in Figure 3 were used with $I_{db} = 0.1$.

part of the total (circuit shown in Figure 1b), pure RC, and diffusion impedance (eq 8) with typical values for the DSC found in photoimpedance measurements (for a 1 cm^2 area electrode).[7,12] One set of curves corresponds to the forward bias case, ($I_{db} = 0.1$) and the other to the small dc current case, ($I_{db} = 10^{-5}$). I_{db} is the differential dc current given by $I_d(V)$ times β. The "$R_PC_PR_s$ circuit" curve corresponds to the circuit in Figure 1b with Z_D replaced by an ohmic resistor, $R_p = 1/I_{db}$. Such a circuit would be the first guess considering the value of the capacitance obtained from the transient photocurrent measurement and the differential resistance of the dark $I-V$ curve. It is evident that the pure RC approximation does not match the total impedance for both bias conditions. The diffusion impedance can be neglected only for currents (I_{db}) smaller than 10^{-5}. In the high current case, ($I_{db} = 0.1$), the imaginary parts of the total and of the diffusion impedance are identical at all frequencies. This means that the effect of the space charge capacitance, C_{SC}, on the total impedance is negligible under forward current flow. As expected, the resistive parts ($R_e(Z)$) of the total and of the RC impedance are converging to the series resistance at very high frequencies and to the forward current resistance at very low frequencies. The rather high value of R_s ($\sim$10 Ω/cm^2) is the cause for an almost $R_PC_PR_s$ equivalent circuit-like shape of the real part of Z. The calculations (Figure 3) show, in agreement with the impedance experiments,[2,8] that very low frequencies in the millihertz regime are indeed required to fully assess the impedance behavior of this type of solar cell. Figure 4 shows the apparent parallel resistance, R_p, and parallel capacitance, C_p, for two different frequencies as a function of the differential forward current, I_{db}. The curves are calculated by transforming the total impedance into an RC-type parallel impedance via $R = [Z]^2/\mathrm{Re}(Z)$ and $C = -\mathrm{Im}(Z)/(\omega[Z]^2)$. If we ignore the series resistance, these values correspond to the assumption of a simple RC analysis.[2,8] At very low frequencies, as usually employed in the experiments (0.1 Hz), the parallel capacitance rises exponentially with $\log(I_{db})$, while the value of the true space charge capacitance (5 μF) is only approached at very low currents. The parallel resistance resembles the differential resistance of the junction at $f = 0.1$ Hz. The dramatic increase in C with forward bias disappears already at the moderate frequency of 1 kHz at which the true space charge capacitance dominates the capacitive behavior.

IV. Discussion

The almost bias-independent capacitance measured in the transient photocurrent experiment (Figure 2) stems from the

SnO_2/TiO_2 back contact in which the photogenerated electrons are separated from their ionic screening charge.[1] This capacitance is a true frequency-independent capacitance in the sense of electrostatics. It relates an inhomogeneous charge distribution to the electric field between these charges ($dC = dQ/V$). The inhomogeneous charge distribution forms the double layer or space charge layer. It is established when the three different materials, SnO_2, TiO_2, and electrolyte, are brought into contact. The physical nature of the transient diffusion capacitance is quite different from that of the space charge capacitance. It is defined in terms of mass transport and not by the stationary charge distribution and corresponding electric field. It is of similar nature as the diffusion capacitance in electrochemistry (Warburg impedance). The *nm*-dimensions of the TiO_2 film and the fact that the high concentration of ionic species screens the electrons in the TiO_2 network on a *nm* length scale make it impossible to assign a large macroscopic electrostatic capacitance to this system. As has been shown in the last section, the experimentally observed apparent supercapacitance under forward bias[2,8] can be easily explained. There is no contradiction to the notion of a narrow charge separating region at the TiO_2/SnO_2 contact with the corresponding space charge capacitance. The physical picture applied here in deriving the expressions for the impedance is the same as the commonly accepted diffusion model for the ac photoresponse of the DSC.[7] The equations describing both types of measurements are of a very similar functional form. Impedance measurements in dependence on the applied forward bias can yield in principle the same information as is obtained from photoimpedance measurements with a variable dc light bias.

It has been argued that the impedance capacitance under high negative bias represents a highly conductive metal-like TiO_2 network. This would result in a Helmholtz layer with a very high surface area corresponding to the inner surface of the nanoporous TiO_2 film.[8] These experiments were carried out, however, in the absence of oxidized species in the electrolyte.[8] Therefore, the electron concentration must have been considerably higher than that in the working solar cell. The diffusion impedance discussed here was not considered as a possible origin of the observed effect. For the working DSC addressed here, the notion of a highly conductive metal-like TiO_2 network can be excluded. The experimental results shown in Figure 2 are in clear contradiction to such an assumption. The metal-like model would also contradict basic considerations concerning the photovoltaic operation of the cell.[1]

The calculated bias dependence (Figure 4) assumes that both electron lifetime and diffusion coefficient are dependent on neither bias nor electron concentration. These assumptions are not correct for the DSC.[12] A realistic $Z-V$ plot with a single set of parameters cannot be obtained if trap filling processes and geometric properties of the TiO_2 network are neglected and if the complicated recombination kinetics are approximated by just a liftime. Improvements in the mathematical description of the impedance could be made in analogy to improved models for the photoimpedance (IMPS, IMVS).[13] Another problem, not touched here, is the current−voltage relationship. The electron concentration at the SnO_2/TiO_2 interface is assumed here to change according to the Boltzmann factor (eq 1); in other words, the forward current is assumed with a diode quality factor of 1. This has never been observed for the DSC. Measured nonideality factors are actually in the range of 2 or even higher. A more realistic description of the forward current would require introducing at least some details concerning the actual recombination reactions in the DSC.

Our aim in this paper is presenting a straightforward physical model that can explain the different capacitive behavior of the DSC as seen in different types of measurements. Insight into the different physical mechanisms that give rise to the apparent different capacitive behavior can indeed be gained from simple analytical models. The one for the diffusion impedance is presented in this paper, the other for the space charge capacitance has been given earlier.[1] A measurement of the latter is presented in this paper (Figure 2). The diffusion length in eqs 7 and 9 is known to vary only slightly with electron concentration.[12] Thus, the model presented here for the diffusion impedance is sufficient for demonstrating the underlying physical mechanism. Experimental results have been published by other authors for the capacitive behavior of the impedance of the DSC under forward bias, though not identified as such.[2] These measurements are in good qualitative agreement with the behavior derived here from a simple physical model for the capacitive behavior of the diffusion impedance in the DSC under forward bias (solid curve, right-hand ordinate, Figure 4).

Acknowledgment. We thank A. J. Frank and J. van de Lagemaat for a discussion during the IPS2000 conference of their measurements shown in ref 2.

References and Notes

(1) Schwarzburg, K.; Willig, F. *J. Phys. Chem. B* **1999**, *103*, 5743.
(2) van de Lagemaat, J.; Park, N.-G.; Frank, A. J. *J. Phys. Chem. B* **2000**, *104*, 2044.
(3) Nazeeruddin, M. K.; Kay, A.; Rodicio, I.; Humphrey-Baker, R.; Müller, E.; Liska, P.; Vlachopoulos, N.; Grätzel, M. *J. Am. Chem. Soc.* **1993**, *115*, 6382.
(4) O'Regan, B.; Graetzel, M. *Nature* **1991**, *353*, 737.
(5) Willig, F. *Ber. Bunsen-Ges. Phys. Chem.* **1988**, *92*, 1312.
(6) Schwarzburg K.; Willig F. *J. Phys. Chem. B* **1997**, *101*, 2451.
(7) Dloczik, L.; Ileperuma, O.; Lauermann, I.; Peter, L. M.; Ponomarev, E. A.; Redmond, G.; Shaw, N. J.; Uhlendorf, I. *J. Phys. Chem. B* **1997**, *101*, 10281.
(8) Zaban, A.; Meier, A.; Gregg, B. A. *J. Phys. Chem. B* **1997**, *101*, 7985.
(9) Shockley, W. *Bell Syst. Tech. J.* **1949**, *28*, 435.
(10) Schwarzburg, K.; Meissner, B.; Willig, F., manuscript in preparation.
(11) Peter, L. M.; Ponomarev, E. A.; Franco, G.; Shaw, N. J. *Electrochim. Acta* **1999**, *45*, 549.
(12) Fisher, A. C.; Peter, L. M.; Ponomarev, E. A.; Walker, A. B.; Wijayantha, K. G. U. *J. Phys. Chem. B* **2000**, *104*, 949.
(13) Schlichthörl, G.; Park, N. G.; Frank, A. J. *J. Phys. Chem. B* **1999**, *103*, 782.